Relationships Between Intense Magnetic Storms Caused By Sheath Regions, CIRs and ICMEs

A. de Lucas, E. Echer, W.D. Gonzalez, L.E.A. Vieira, L.F. Guarnieri, A. Dal Lago, M.R. da Silva, J.C. dos Santos – Instituto Nacional de Pesquisas Espaciais - INPE/MCT, São Jose dos Campos/SP, Brazil, and N.J. Schuch – Centro Regional Sul de Pesquisas Espaciais -.CRSPE/INPE/MCT, Santa Maria/RS, Brazil.

Abstract

In this work we study comparatively intense magnetic storms (Dst < -100 nT) caused by Corotating Interaction Regions (CIRs), or by interplanetary coronal mass ejection (ICMEs), or by sheath regions. Our aim is to analyze their interplanetary characteristics (electric field Ey, Bs interplanetary magnetic field) and their energy coupling function, (ε), and the total energy input, (W_ε), to analyze the differences between events caused by different interplanetary structures. The geomagnetic data/indices are also employed to study the ring current dynamics and to search for the differences in the storm evolution in these events. The selected storms are 10 March 1998, 6 August 1998, 17 April 1999, 22 September 1999, 24 May 2000, and 6 de November 2000. The interplanetary data were obtained from ACE spacecraft's Web page, and the geomagnetic data is from World Data Center for Geomagnetism - Kyoto (WDC-Kyoto) and from Space Physics Interactive Data Resource, on the NOAA's Web page.

Introduction

For space weather forecasts and proper understanding of the magnetospheric phenomena the reliable solar wind measures are crucial. When we study the magnetic storm phenomena it is essential to analyze the characteristics of this ionized gas because the structures and the solar magnetic field are traveling in the interplanetary space with it. Due the direction and variability of the interplanetary magnetic field (IMF), it is the most important parameter to analyze the dynamics of the magnetosphere: the IMF southward has an extremely significant role in the injection of energy due the reconnection process that is a controlling factor for energy and plasma input across the boundary (Dungey et al., 1961).

The total energy input into the magnetosphere is dissipated by different forms. It is partially deposited in the inner magnetosphere, forming the ring current belt, but this energy represents some part of the total entry energy. Another part is deposited in the auroral ionosphere as heat energy – due the Joule heating and the impact of auroral particles (Akasofu, 1981).

Our aim is to determine the entry and consumption energy during intense magnetic storm events caused by different structures.

Data Selection

In order to make the study of the magnetospheric response during intense magnetic storm caused by CIRs, ICMEs, and sheath region, we have taken events from 1998 to 2000, how it can be seen on Table 1. In these epochs the solar data of ACE spacecraft are evaluated.

Date	t_{main}	Dst_p	AE_p	$K_{p\,max}$	t
CIR 10/03/1998	10h	-116	1594	7_0	5(3)
SHEATH+CIR 6/08/1998	12h	-169	1921	7_0	4(2)
SHEATH+CIR 24/05/2000	7h	-147	1858	8_0	5(3)
ICME 17/04/1999	13h	-105	1391	7_0	2(0)
ICME 22/09/1999	4h	-164	1877	8_0	7(5)
ICME 06/11/2000	12h	-159	2033	7_0	-3(-5)

Table 1: Some characteristics of the selected events: on the first column is the occurrence date of the intense magnetic storm, after that the main phase duration, and the *Dst*, AE and K_p indices peak values. The last column is the delay time between the peak negative values of B_s and Dst index.

The instrumentation on boarding ACE spacecraft, responsible to the solar wind plasma and IMF measures and shocks detection, is SWE (Faraday Cup Solar Wind Experiment) and MFI (Magnetic Field Instrument) sensors. The data selection on the time to analyze the interplanetary characteristics is very important in order to study the response of the magnetosphere.

Interplanetary Structures Causing the Magnetic Storms

The solar wind at low heliograph latitudes tends to be structured into alternating streams of high and low speed flows that corotate with the Sun (*Gosling et al.*, 1995b), while in high latitudes prevails a nearly constant wind with speed and density about 750 km/s and 2.5 cm^{-3}, respectively (*Phillips et al.*,1994). We can see in Figure 1 that the interaction between two kinds of solar wind streams results in a compression region. When the solar wind is sometimes stationary the compression region rotates with the Sun.

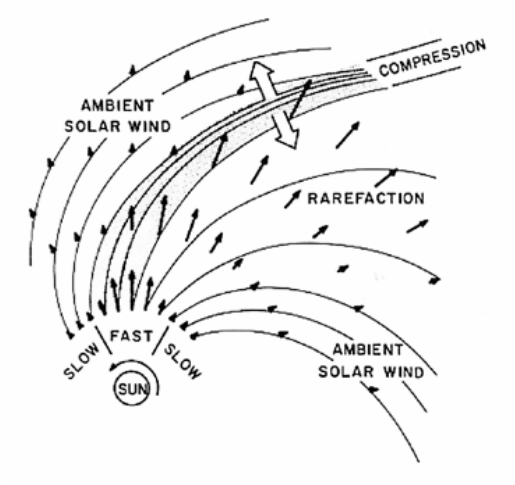

Figure 1 – The ambient solar wind interacting with the high-speed solar wind and forming the compression and rarefaction regions (from *Pizzo*, 1985).

The CIRs is a region of the high pressure because of compressed plasma due the interaction between high-speed and the precedent slow solar wind (*Smith and Wolfe*, 1976; *Balogh*, 1999). Its leading edge is a forward wave that propagates into the slow solar wind ahead of a high-speed stream, while the trailing edge is a reverse wave that propagates back into the stream itself. (*Gosling and Pizzo*, 1999). Between the boundaries the density tends to be relatively low, while that ahead of the stream and in the rising portion of the stream tends to be relatively high. These density transitions generally occur abruptly in the same time when the velocity increases quickly. Within the CIR the proton temperature and magnetic field strength increase, and the solar wind speed rises (*Balogh et al.*, 1999). The magnetic polarity within this stream is essentially constant (*Burlaga*, 1995).

Another kind of interplanetary structures is a magnetic cloud (MC). Magnetic clouds are a subgroup of the coronal mass ejections. During the passage of this structure the magnetic field direction varies slowly, the intensity of this field increases, and plasma temperature and thermal pressure decrease, i.e., there is a low-beta plasma. Another hand, the velocity decreases as the magnetic cloud passes. There is a smooth rotation of the IMF vector within the magnetic cloud structure (*Burlaga et al.*, 1981).

Magnetospheric activity is often generated by southward IMF in a region piled-up solar wind plasma in front of CME ejecta called the sheath region (*Tsurutani et al.*, 1988). In this region the solar wind plasma is heated and compressed and the draping of the CME ejecta can cause intense southward B_z events.

In many cases spacecraft upstream of the Earth observe only a shock followed by a disturbed solar wind flow (i.e. post-shock stream) but the CME ejecta itself is missed. Practically all interplanetary shocks observed at 1 AU have been demonstrated to be driven by CMEs (*Sheeley et al.*, 1985), whereas the CIRs developed shocks mainly at larger distances from the Sun. It can make a big difference which type of solar wind structure causes the storm (*Huttunen and Koskinen*, 2004).

We investigated six cases in more detail to see the differences in the energy entry and consumption during storms driven by different solar wind structures.

Transference of Energy

Generally, the direction of the interplanetary magnetic field (IMF) is the regulator of the energy transference to the magnetosphere. When the IMF is southward, magnetic flux is transferred from dayside magnetosphere to geomagnetic tail (e.g. *Baker et al.*, 1984). And this direction is an important parameter to calculate the energy input.

In the coupling electromagnetic the energy of the solar wind enters partially into the magnetosphere. This rate is given by the solar wind-magnetosphere coupling parameter ε (erg/s), proposed by Perreault and Akasofu (1978):

$$\varepsilon = l_0^2 V B^2 \sin^4\left(\frac{\theta}{2}\right) \quad (1)$$

where $\mathrm{V}(\mathrm{cm}/s)$ is the solar wind bulk speed, $\mathrm{B}(\gamma)$ is the IMF magnitude, θ is the angle between the GSM z-direction and the IMF projection in the y-z plane. The integral of epsilon parameter, $W_\varepsilon(J)$, represents the energy stored in the magnetotail.

To estimate the dissipated energies in the magnetosphere we use two geomagnetic indices, the *Dst* and AE indices, where the *Dst* index gives the average magnetic field intensity of the ring current. Here we remove the contribution from other current systems than ring current to the Dst measure, mainly by the Chapman-Ferraro current (*Turner et al.*, 2001), and we use their contributions to estimate the ring current energy with the DPS (Dessler-Parker-Sckopke) relation. *Burton et al.* (1975) suggested the correction of the form $Dst^* = Dst - b\sqrt{P_{SW}} + c$, where $b = 7.26\,nT(nPa)^{-1/2}$, $c = 11.0nT$ (*O'Brien and McPherron*, 2000), and P_{SW} is the solar wind dynamic pressure.

On the other hand, the ring current energy can be estimated by using the ground-based Dst index, which has been associated with the total energy in the ring current particles (Dessler and Parker, 1959; Schopke, 1966).

$$Dst^{*} = \frac{\mu_0}{2\pi} \frac{W_{RC}}{B_0 R_E} \quad (2)$$

Here the kinetic energy of the ring current particles is given by W_{RC}, B_0 .is the equatorial magnetic field strength, and μ_0 is the permeability of free space.

According to *Akasofu's* (1981) formulation the energy consumption rate in the Earth's ionosphere is given by the sum of the kinetic power of the auroral particles, being lost in the ionosphere due the precipitation, $P_A(erg/s) = 10^{15} AE(nT)$, and of the Joule heating, $P_J(erg/s) = 2\times10^{15} AE(nT)$, associated with electric current flow (Belehaki and Tsagouri, 2001). So, the energy lost in the ionosphere is given by

$$P_I = P_A + P_J \quad (3)$$

After that, we want to determine the entry and consumption energy during CIRs, ICMEs, and sheath regions events, remembering the total energy lost is given by the sum of ionosphere and ring current energy consumption, i.e.,

$$W_L = W_I + W_{RC} \quad (4)$$

Event from 23 to 27 of May, 2000

Figure 2 shows, at 23 UT on 23rd May, 2000, a shock was detected at 1AU. Behind this shock a sheath region was formed. The southward magnetic field stayed for 1 hour with values below -10nT, and the electric field remained above 10mV/m for 1 hour. After that, a CIR arrived at 12 UT on the day after the shock, and ended at 16 UT on 24th May.

We can observe many fluctuations on southward IMF component, which caused the horizontal component of geomagnetic field to reach a peak value of -147nT, and peak Kp equal to 8_0. During 7 hours there was injection on the ring current until the time where the phase recurrent took place.

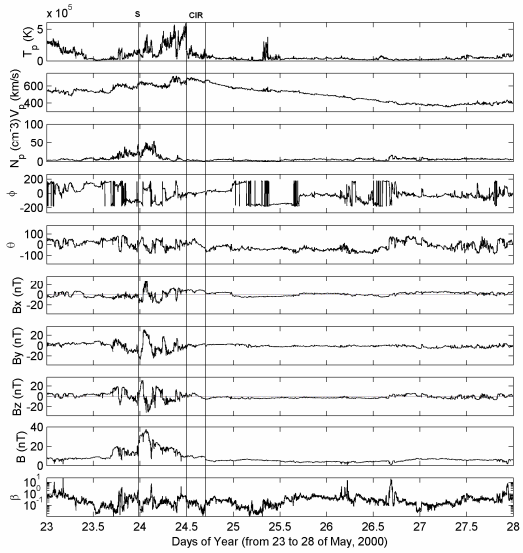

Figure 2 - The storm was caused by a CIR on 24th May 2000. From top to bottom: proton temperature, T_p; proton speed, V_p; proton density, N_p; azimuthal angle, ϕ, latitudinal angle, θ, IMF components, B_x, B_y, and B_z, IMF intensity, B, and β. This data was taken from ACE satellite in a time interval of 64s.

Event from 21 to 27 of September, 1999

The solar origin of this event was a CME on 20th September (0606 UT) released from the Sun to the medium interplanetary. Figure 3 shows at 1AU at 1222 UT on 22nd of September a shock was detected. The ICME started on 22nd September (19 UT) and ended on 24th September (18 UT). There were low-beta proton, the IMF intensity around ~35 nT, a strong IMF rotation of Bz remaining below -10nT for 2 hours, and the proton temperature was slightly reduced. Within the structure the proton density was bigger than ahead.

The Dst index had a maximum negative value of -173 nT, the Kp=8_0, and the auroral eletroject index arrived values around 2000 nT during the storm main phase. During an interval of 3 hours, the electric field remained above 5mV/m, increasing the ring current injection and contributing to the deflection of horizontal geomagnetic field.

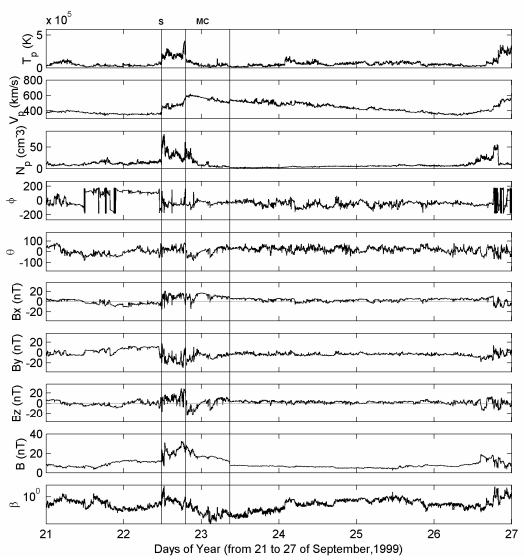

Figure 3 - The storm was caused by an ICME on 23rd September 1999. From top to bottom: proton temperature, T_p; proton speed, V_p; proton density, N_p; azimuthal angle, ϕ, latitudinal angle, θ, IMF components, B_x, B_y, and B_z, IMF intensity, B, and β. This data was taken from ACE spacecraft in a time interval of 64s.

Results

Variations on the solar wind speed and the IMF strength and direction mean that interaction with the magnetosphere and ionosphere is highly episodic in its strength and duration (e.g., *Nishida*, 1983; *Baker*, 1997). When the episodes of solar wind-magnetosphere are longer and more energetic they give rise to major magnetic storms. Here we have calculated the energy input into the magnetosphere during the main phase and from the initial time when the main phase start until the *Dst* get variations of 50 and 100 nT, of each event of the intense magnetic storm, as it is shown in Table 2. The solar wind energy coupling rate was calculated by the epsilon parameter which is determined assuming the reconnection is the responsible process.

Magnetic Storms	$\int \varepsilon dt$ (J)	$\int \varepsilon dt$ (J) (50 nT)	$\int \varepsilon dt$ (J) (100 nT)
CIR 10/03/1998	2.89×10^{16}	2.71×10^{16}	2.89×10^{16}
SHEATH+CIR 6/08/1998	6.11×10^{16}	4.98×10^{16}	6.11×10^{16}
SHEATH+CIR 24/05/2000	4.32×10^{16}	3.08×10^{16}	3.58×10^{16}
ICME 17/04/1999	1.22×10^{16}	2.09×10^{14}	6.51×10^{15}
ICME 22/09/1999	1.94×10^{16}	1.69×10^{16}	1.94×10^{16}
ICME 06/11/2000	2.98×10^{16}	1.86×10^{16}	2.75×10^{16}

Table 2 - In this table is shown the integrated coupling parameter during the main phase, and when the Dst variation get of 50 and 100 nT. On the last two columns, the initial time is the instant when the main phase starts, and the final time is the time when Dst assumes the variations above. All energies are given in Joules.

On Table 3, we compare the solar wind energy which was accumulated in the two tail lobes and how many this energy was dissipated by (1) Joule heating, (2) precipitating particles, and (3) enhancement of the trapped particle population in the ring current.

Magnetic Storms	W_ε (J)	W_L (J)
CIR 10/03/1998	2.89×10^{16}	3.1×10^{16}
SHEATH+CIR 6/08/1998	6.11×10^{16}	2.8×10^{16}
SHEATH+CIR 24/05/2000	4.32×10^{16}	4.69×10^{16}
ICME 17/04/1999	1.22×10^{16}	1.29×10^{16}
ICME 22/09/1999	1.94×10^{16}	2.0×10^{16}
ICME 06/11/2000	2.98×10^{16}	5.48×10^{16}

Table 3 – Total energy dissipated during the main phase of each magnetic storm event. The first column indicates each magnetic storm event, the second column is the ring current energy input, and the last column is the lost energy due the Joule heating and precipitation.

Conclusions

During sheath regions-storms there was more solar wind energy inputting into the magnetosphere than the CIR and ICME-storms. This can be caused because the IMF-B_z component is highly turbulent within the sheath regions and sometimes is intensified again due another shock.

We can see on Table 2, for ΔDst = 50, the energy input was in general was greater for the sheath regions than CIR and ICMEs-storms, i.e., ICME and CIR are more

geoeffective than sheath regions because it is necessary more energy inputting into the magnetosphere to cause the same variation on Dst index. To variations of 100 nT, only an ICME-storm had a greater value than other events, but in general sheath regions-storms had a higher values than the events caused by other structures.

When we observe the lost energy and we comparing with the entry energy calculated by the epsilon parameter we conclude that the consumption energy exceeds the coupling parameter in almost every cases, i.e. the epsilon parameter is only an indicator of the total energy which entries in the magnetosphere during the reconnection process occurs.

The time interval between Bz negative peak and Dst index peak was shorter during the 16th April, 1999 event and 24th May, 2000 both caused by MC/ICMEs, how is shown in Table 1. The 22nd September, 1999 storm caused by an ICME too presented time delay of 5h between the peaks of Bs and Dst which is the longer. This effect occurs probably because the long rotation of the magnetic field within the magnetic cloud. These times were calculated considering that the time necessary to solar wind come from the satellite to dayside magnetosphere is about 1h, and that the magnetospheric response time is around 1h.

Acknowledgments

The authors would like to acknowledge the Instituto Nacional de Pesquisas Espaciais/INPE-MCT and to Brazilian government agency CNPQ for master fellowship. In the same manner the authors would like thank to World Data Center for Geomagnetism –Kyoto, and Space Physics Interactive Data Resource for the geomagnetic data, to the International Solar Terrestrial Physics Project, through ACE teams for high-resolution solar wind data and to the National Space Science Data Center (NASA/Goddard) for the OMNI data set.

References

Akasofu, S-I, 1981. Energy coupling between the solar wind and the magnetosphere, **Space Sci. Rev. 28**, 121p.

Baker, D.N., Bame, S.J., Belian, R.D., Feldman, W.C., Gosling, J.T., Higbie, P.R., Hones Jr., E.W., McComas, D.J., Zwickl, R.D., 1984. Correlated dynamical changes in the near-Earth and distant magnetotail regions: ISEE3. **J. Geophys. Res. 89**, 3855-3864p.

Baker, D.N., 1997. A quantitative assessment of energy storage and release in the Earth's magnetotail, **J. Geophys. Res. 102**, 7159-7168p.

Baker, D.N., N. E. Turner, T. I. Pulkkinen, 2001. Energy transport and dissipation in the magnetosphere during geomagnetic storms, **J. Atmosph. Sol-Terr. Phys, 63**, 421-429p.

Balogh, A., 1999. The Solar Origin of Corotating Interaction Regions and Their Formation in the Inner Heliosphere. **Space Sci. Rev., 89**, 141.

Belehaki, A., Tsagouri, I., 2001. Magnetosphere energetics during substorms events: IMP-8 and GEOTAIL observations, **J. Atmosph. Sol-Terr. Phys., 63**, 657p.

Burlaga, L.F., Sittler, E., Mariani, F., Schwenn, R., 1981. Magnetic loops behind an interplanetary shock: Voyager, Helios, and Imp-8 observations, **J. Geophys. Res., 86,** 6673p.

Burlaga, L.F., 1995. **Interplanetary Magnetohydrodynamics**. Oxford University Press, New York.

Dessler, A., J., Parker, E.N., 1959. Hydromagnetic theory of geomagnetic storms, **J. Geophys. Res., 64**, 2239p.

Dungey, J.W., 1961. Interplanetary magnetic field and the auroral zones, **Phys. Rev. Lett.**, 6, 47p.

Gonzalez, W. D., Tsurutani, B., Clua de Gonzalez, A. L. , 1999. Interplanetary origin of geomagnetic storms, **Space Sci. Rev., 88**, 529-562p.

Gosling, J. T., Bame, S. J., Feldman, W. C., McComas, D. J., Phillips, J. L., Goldstein, B. E., Neugebauer, M., Burkepile, J., Hundhausen, A.J., Acton, L.,1995b. The band of solar wind variability at low heliographic latitudes near the solar activity minimum: Plasma results from the Ulysses rapid latitude scan, **Geophys. Res. Lett., 22,** 3329-3332p.

Gosling, J. T., Pizzo, V. J., 1999. Formation and evolution of corotating interaction regions and their three dimensional structure, **Space Sci. Rev., 89,** 21-52p.

Huttunen, K. E. J., Koskinen, H. E. J., 2004. Importance of post-shock streams and sheath region as drivers of intense magnetospheric storms and high-latitude activity, **Ann. Geophys., 22**, 1729-1738p.

Nishida, A., 1983. IMF control of the Earth's magnetosphere, **Space Sci. Rev., 34,** 185p.

O'Brien, P., McPherron, R.L., 2000. An empirical phase space analysis of ring current dynamics: Solar wind control of injection and decay, **J. Geophys. Res., 105**, 7707p.

Perreault, P., Akasofu, S-I, 1978. A study of geomagnetic storms. **Geophys. J. Royal Astron. Soc. 54**, 574-573p.

Phillips, J. L., Balogh, A., Bame, S. J., Goldstein, B. E., Gosling, J. T., Hoeksema, J. T., McComas, D. J., Neugebauer, M., Sheeley, N. R., Wang, Y.-M., 1994. Ulysses at 50° South: Constant Immersion in the high-speed solar wind. **J. Geophys. Res., 21,** 1,105-1,108p.

Richardson, I.G., Cane, H.V., 2003. Interplanetary coronal mass ejections in the near-Earth solar wind during 1996-2002, **J. Geophys. Res., 108**, 1156p.

Sckopke, N., 1966. A general relation between the energy of trapped particles and the disturbance field near the Earth, **J. Geophys. Res., 71**, 3125p.

Smith, E. J., Wolfe, J. H., 1976. Observations of interaction regions and corotating shocks between one and five AU: Pioneers 10 and 11, **J. Geophys. Res., 3,** 137-140p.

Turner, N.E., Baker, D.N., Pulkkinen, T.I., Roeder, J.L., Fennel, J.F., Jordanova, V.K., 2001. Energy content in the stormtime ring current, **J. Geophys. Res., 106**, 19149p.